

Optical Measurement of the Effect of Electric Fields on the Nuclear Spin Coherence of Rare-Earth Ions in Solids

R. M. Macfarlane,^{1,*} A. Arcangeli,^{2,†} A. Ferrier,^{2,3} and Ph. Goldner^{2,‡}

¹IBM Almaden Research Center, 650 Harry Road, San Jose, California 95120, USA

²PSL Research University, Chimie ParisTech—CNRS, Institut de Recherche de Chimie Paris, 75005 Paris, France

³Sorbonne Universités, UPMC Université Paris 06, 75005, Paris, France

(Received 30 April 2014; published 7 October 2014)

We show that the coherence properties of the nuclear spin states of rare-earth ions in solids can be manipulated by small applied electric fields. This was done by measuring the Stark effect on the nuclear quadrupole transitions of ^{151}Eu in Y_2SiO_5 (YSO) using a combination of Raman heterodyne optical detection and Stark modulated quadrupole echoes to achieve high sensitivity. The measured Stark coefficients were 0.42 and 1.0 Hz cm/V for the two quadrupole transitions at 34.54 and 46.20 MHz, respectively. The long decoherence time of the nuclear spin states (25 ms) allowed us to make the measurements in very low electric fields of ~ 10 V/cm, which produced 100% modulation of the nuclear spin echo, and to measure Stark shifts of ~ 1 Hz or 20 ppm of the inhomogeneous linewidth.

DOI: 10.1103/PhysRevLett.113.157603

PACS numbers: 76.60.Gv, 71.70.Ej, 76.30.Kg, 76.60.Lz

Nuclear spin levels of rare-earth ions in solids are very attractive candidates for q -bits in quantum memories and other quantum information applications because of their long coherence times T_2 . Using nuclear spins in open shell ions with narrow optical resonances, such as rare earths (RE), introduces the possibility of using sensitive optical detection schemes to measure nuclear spin coherence and also of transferring coherence between nuclear and electronic states. The importance of RE doped crystals for quantum information processing is shown by recent demonstrations of quantum memories for light [1–3], entanglement storage [4,5], light matter teleportation [6], as well as single ion detection [7] and coherent manipulation [8]. Moreover, it has been found that the coherence times of nuclear spin states can be greatly extended by the application of specific external magnetic fields or the application of specific rf pulse sequences [9–11]. We show here that it is also possible to exercise control over the coherence properties of RE nuclear spins with electric fields (Stark effect [12]). A combination of electric field induced spin-echo modulation and optical Raman heterodyne detection [13] was used to measure the Stark effect of the nuclear quadrupole levels of dilute Eu^{3+} ions in Y_2SiO_5 with high sensitivity using electric fields of only ~ 10 V/cm. To the best of our knowledge this is the first observation of the Stark effect on nuclear levels of RE ions, and the first application of optical techniques to the measurement of the Stark effect of nuclear states. Our measurements combine Raman heterodyne detection of NQR with the exquisitely sensitive Stark echo modulation technique introduced by Mims [14] in the context of electron paramagnetic resonance. Subsequently the technique was used in nuclear quadrupole echo measurements [15]. The sensitivity of Stark echo modulation derives from the long decoherence

times of quantum states. In the case of the quadrupole levels of ^{151}Eu these are 25 msec at 4 K. We were able to easily resolve Stark shifts of 0.6 Hz or ~ 20 ppm of the inhomogeneous linewidth of the transitions, and measure Stark coefficients of less than 1 Hz cm/V using electric fields of ~ 10 V/cm. The mechanism for the nuclear Stark effect is coupling of the nuclear quadrupole moment to the change in the crystalline electric field gradient produced by the applied field [16,17]. We also used the Stark echo modulation technique to measure the optical Stark effect which is $\sim 10^4\times$ larger and measures the vector difference between the ground and excited electric dipole moments.

Y_2SiO_5 (YSO) is a monoclinic crystal with space group C_{2h}^6 and eight formula units per unit cell. The Eu^{3+} ions substitute for Y^{3+} ions on two crystallographic sites of C_1 symmetry. Europium has two isotopes: ^{151}Eu (44.77%) and ^{153}Eu (52.23%), with quadrupole moments of +0.95(10) eb and +2.42(20) eb, respectively [18]. The ratio of the quadrupole moments is known more precisely from laser ion-beam spectroscopy as 2.5516(6) [19]. The nuclear quadrupole levels of the 7F_0 ground state of Eu^{3+} are described by the Hamiltonian

$$H = (P + P_{pq})[I_z^2 - I(I+1)/3 + (\eta/3)(I_x^2 - I_y^2)]. \quad (1)$$

Here, I is the nuclear spin, P the pure quadrupole interaction between the nuclear quadrupole moment and the electric field gradient resulting from the distribution of lattice ions and the $4f$ electrons of the Eu^{3+} ion and η is the asymmetry parameter. The pseudo-quadrupole interaction P_{pq} [20] originates in the second order magnetic hyperfine interaction through the 7F_1 level. Deviations of the ratio of the quadrupole splittings of the two isotopes $(P + P_{pq})^{153}/(P + P_{pq})^{151}$ from the bare value of 2.5516 gives a measure

of the size of the pseudo-quadrupole contribution. In general, for Eu^{3+} ions in solids this contribution ranges from about 1%–5%. In YSO the ratio of the quadrupole splittings is 2.58 and the pseudo-quadrupole contribution is at the lower end of this range so the dominant mechanism for the observed Stark shifts comes from the modification of the EFG by the applied electric field and we neglect P_{pq} from now on. The Stark shifts for the ^{153}Eu isotope will be larger than those measured here for ^{151}Eu by a factor of 2.6.

The ^{151}Eu nucleus has a spin $I = 5/2$ and the quadrupole splittings are shown in Fig. 1 and labeled by their dominant spin components. For the ground state, $P = 12.4$ MHz and $\eta = 0.661$ [21], and for the 5D_0 excited state, $P = 27.3$ MHz and $\eta = 0.644$ [22]. The order of the hyperfine components shown in Fig. 1 is that determined for ^{153}Eu by Lauritzen *et al.* [23]. The Stark shifts of these resonances were measured using the echo modulation technique [14]. A voltage pulse of length t' and amplitude V_s , applied across the crystal of thickness d , produces an electric field $E_s = V_s/d$ along the $D1$ axis during the time interval t_{12} between the echo excitation pulses as shown in Fig. 2(a). Because of the centrosymmetric space group, equal and opposite phase shifts are induced between sets of inequivalent ions related by inversion. In YSO for $E_s \parallel D1$ there are 2 such sets of ions and a single modulation curve is obtained with exact nulls at odd multiples of π in the electric field induced phase shift $2\Omega t'$ [24]. The echo intensity I_{ech} is given by

$$I_{\text{ech}} = \frac{1}{2} I_0 [1 + \cos(2\Omega t')], \quad (2)$$

where Ω is the frequency shift produced by the interaction of the nuclear quadrupole moment with a linear change in EFG induced by the applied electric field [17]. YSO is not piezoelectric, so the electric field does not induce a crystal strain and acts only to change the EFG Δq , such that the ij th component

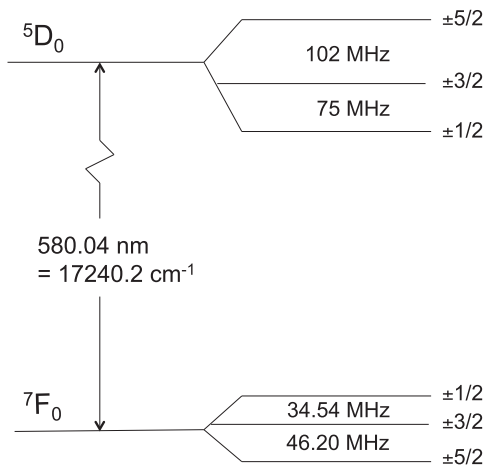


FIG. 1. Energy levels for $^{151}\text{Eu}^{3+}$ in site 1 of YSO showing the nuclear quadrupole splittings.

$$\Delta q_{ij} = \sum_{k=x,y,z} R_{ijk} E_s^k, \quad (3)$$

is related to the k th component of the applied electric field E_s by the third rank tensor R_{ijk} which expresses the effect of the electric field on the EFG. For the low C_1 site symmetry of the Eu ion in YSO the tensor R has 15 nonzero elements. Here we only determine the Stark shifts for E_s along the $D1$ axis. The parameters P and η in Eq. (1) express the interaction of the quadrupole moment of Eu with the EFG in the absence of the external electric field. The effect of the electric field can be phenomenologically described by adding terms δP and $\delta\eta$ to P and η . In nonaxial sites such as in YSO, the electric field affects both P and the asymmetry parameter η , so the change in the quadrupole splittings is not proportional to the splitting, whereas in axial symmetry only one parameter P , describes the quadrupole splitting and the Stark shifts are expected to be proportional to these splittings for E_s parallel to the symmetry axis and zero perpendicular to it [15].

For the optical transition, the frequency shift is given by

$$\Omega = 2\pi[(\vec{\mu}_e - \vec{\mu}_g)/\hbar] \cdot \vec{E}_s = \delta\vec{\mu} \cdot \vec{E}_s/\hbar, \quad (4)$$

where $\delta\vec{\mu}$ is the vector difference between the dipole moments of the ground and excited states.

A sample of 0.1% Eu:YSO $10 \times 5 \times 1$ mm with the $D1$ axis perpendicular to the 5×10 mm faces was mounted in a cryostat in helium gas at 4.5 K. Thin brass electrodes were attached to the 5×10 mm crystal faces with silver paste and the sample was oriented so that the static electric field E_s , external magnetic field H_0 , and the incident laser polarization E_L , were parallel to the $D1$ axis and light from a ring dye laser with a linewidth of ~ 1 MHz propagated

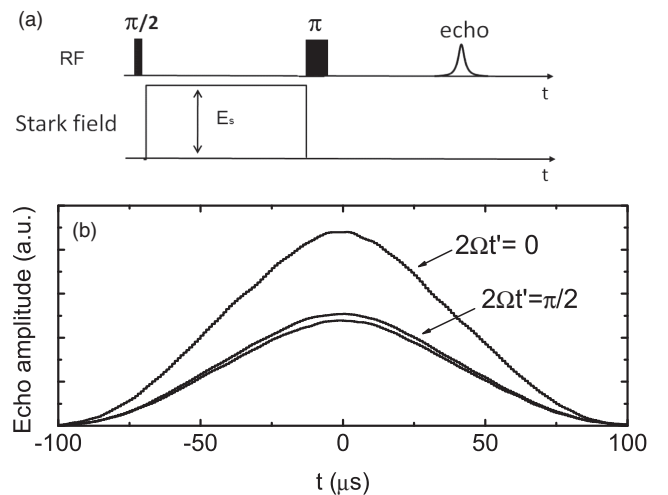


FIG. 2. (a) Stark echo pulse sequence. (b) Echo signals on the 34.54 MHz transition for phase shifts of zero and close to $\pi/2$. Near $2\Omega t' = \pi/2$, a frequency shift of 0.6 Hz for a change in field of 1.4 V/cm is clearly resolved.

along the coil and b axes. The ${}^7F_0 - {}^5D_0$ transition of Eu^{3+} ions in site 1 of YSO had a linewidth of 2.2 GHz, a peak absorption coefficient of 2.4 cm^{-1} for light polarized along $D1$, and a vacuum wavelength of 580.04 nm ($=17\,240.2 \text{ cm}^{-1}$). The sample was inserted into a 5-turn coil 15 mm long and 5 mm in diameter.

The Raman heterodyne process involves three levels—in this case two nuclear quadrupole levels in the ground 7F_0 state (1,2) and one in the excited 5D_0 state (3). Detection of nuclear quadrupole resonance was carried out both in cw and pulsed (echo) modes. The square of the amplitude of the heterodyne beat signal is proportional to $\chi_1 \chi_2 \chi_3 (\rho_{22} - \rho_{11})$ [13], where χ_1, χ_2, χ_3 are the Rabi frequencies for the transitions $1 \rightarrow 2$ (rf), and $1 \rightarrow 3$ and $2 \rightarrow 3$ (optical), respectively, and $(\rho_{22} - \rho_{11})$ is the population difference between the two quadrupole levels. This nonthermal population difference was created by an optical pumping preparation cycle. The laser was off during the rf spin-echo sequence. Consideration of the symmetry properties of the four components of the nonlinear susceptibility contributing to the total Raman heterodyne signal: $\chi_{xxx}, \chi_{yyz}, \chi_{xyz}, \chi_{yxz}$ [25] shows that no cancellation occurs for our configuration. For cw measurements of the inhomogeneous linewidths of the quadrupole transitions of Eu^{3+} ions in site 1, 4 W of rf were applied to the coil and demodulated signals of $\sim 1 \text{ V}$ were averaged to get a S/N of $\sim 20:1$. Linewidths of the 34.54 and 46.20 MHz transitions of ${}^{151}\text{Eu}^{3+}$ were 20 and 38 kHz, respectively.

From nutation measurements on the 34.54 MHz transition, the length of a π pulse was $75 \mu\text{sec}$. The echo excitation pulses were separated by $t_{12} = 10 \text{ ms}$, and the Stark pulse length was $t_{12} - 50 \mu\text{s}$ so that it did not overlap the rf pulses. Because of the sensitivity of the Stark modulation technique, fields of only tens of V/cm were required. Typically 150 shots were averaged at a rate of 5 Hz. Figure 2(b) shows an echo signal in the absence of an electric field and for a field producing a phase shift $2\Omega t' = \pi/2$ where the change in echo intensity as a function of phase shift is a maximum. We were able to easily resolve a Stark shift of 0.6 Hz or $\sim 20 \text{ ppm}$ of the inhomogeneous linewidth of the transition, for a change in electric field of 1.4 V/cm. The dependence of the quadrupole echo intensity on the applied field is shown in Fig. 3(a). The data show the $\cos(2\Omega t')$ dependence expressed in Eq. (2), with the first null at $2\Omega t' = \pi$. The frequency shift $\Omega/2\pi$ can be obtained by rearranging Eq. (2) and is shown in Fig. 3(b). The shift is linear in the applied electric field as expected for a noncentrosymmetric site and the magnitude of the shift is 0.43 Hz/cm/V.

Measurements with the same time delays were made on the 46.20 MHz transition. Figure 4(a) shows the echo intensity as a function of the applied voltage together with a fit to Eq. (2). The inferred frequency shift as a function of electric field is plotted in Fig. 4(b) and the slope gives the Stark shift of 1.0 Hz/cm/V. These Stark coefficients are

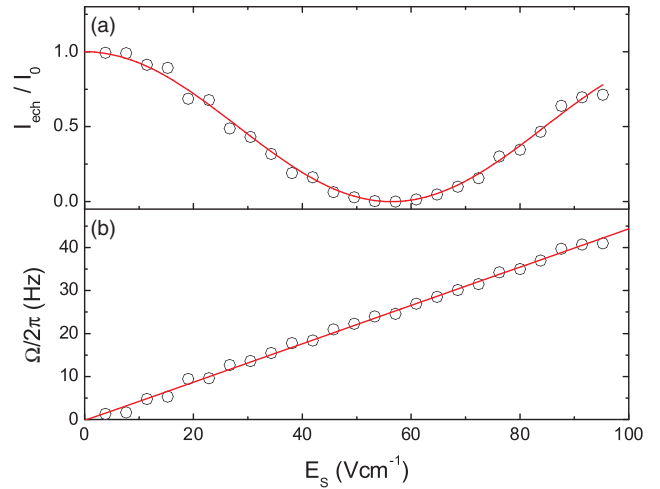


FIG. 3 (color online). (a) Dependence of the nuclear quadrupole echo intensity on electric field (circles) for the 34.54 MHz transition showing the null at a phase shift of π ($E_s = 57 \text{ V/cm}$) with fit to Eq. (2) (line). (b) Stark shift of the transition frequency as a function of the Stark field (circles). A linear fit gives a slope of 0.43 Hz/cm/V.

comparable in magnitude with those measured in non-transition compounds for nuclei with similar quadrupole moments [15].

Our measurements give the absolute values of the Stark coefficients for the two quadrupole transitions. This does not uniquely determine δP and $\delta \eta$. A measurement of the $\pm 1/2$ to $\pm 5/2$ transition at 80 MHz would provide the relative sign of the shifts but we could not observe that resonance. The values of δP and $\delta \eta$ were determined using a MATLAB function that solved for the spin Hamiltonian

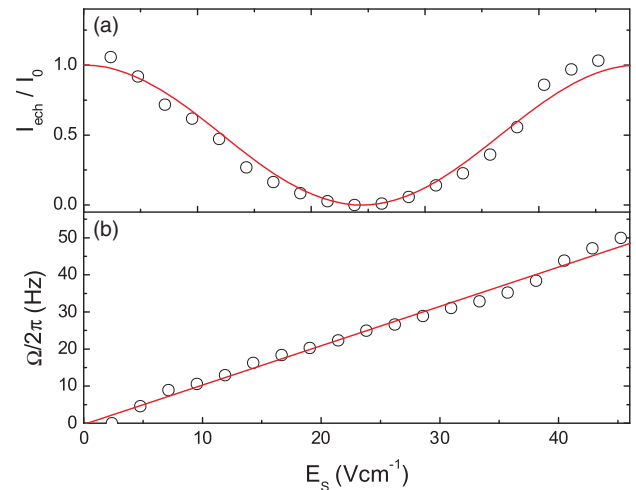


FIG. 4 (color online). (a) Dependence of the nuclear quadrupole echo intensity on electric field for the 46.20 MHz transition showing the null at a phase shift of π ($E_s = 24 \text{ V/cm}$). (b) Stark shift of the transition frequency as a function of the Stark field (circles). A linear fit gives a slope of 1.0 Hz/cm/V.

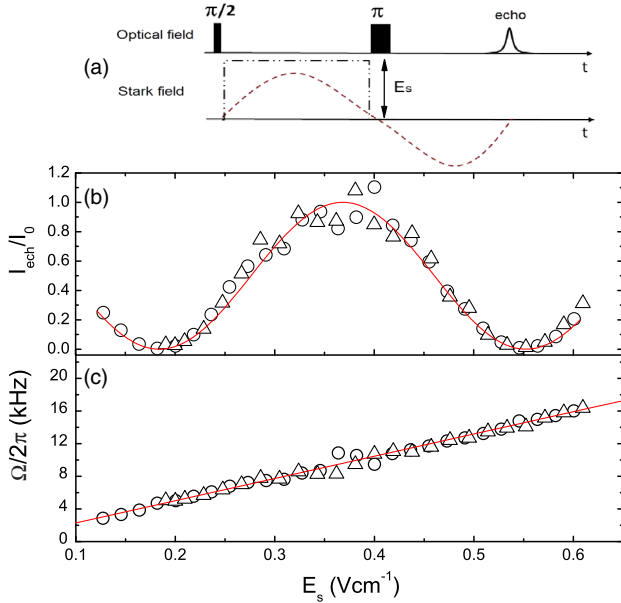


FIG. 5 (color online). (a) Optical and Stark pulse sequences showing the sine and rectangular electric-field functions. To have equal integrals of the absolute values of the electric field, the amplitude of the sine field was $2E_s/\pi$. (b) Dependence of the photon echo amplitude on electric field for the $17\,240.2\text{ cm}^{-1}$ transition for the rectangular (circles) and sine (triangles) pulses showing the nulls at phase shifts of π and 3π . (c) Stark shift of the transition frequency. A linear fit gives a slope of 27 kHz cm/V .

parameters given the Stark shifted frequencies of the two quadrupole transitions. Let the signs of the Stark shifts for the (46.2, 34.54 MHz) transitions be designated (+, +), (-, -), (+, -), and (-, +). Then the corresponding values of $(\delta P, \delta \eta)$ per unit electric field, i.e., 1 V/cm are $(-0.25\text{ Hz}, -0.10 \times 10^{-7})$, $(0.25\text{ Hz}, 0.10 \times 10^{-7})$, $(-0.19\text{ Hz}, -0.38 \times 10^{-7})$, $(0.19\text{ Hz}, 0.38 \times 10^{-7})$, respectively.

In addition to the quadrupole echoes we measured a photon echo in the same geometry. Echo excitation pulses were created with an acousto-optic (A-O) modulator. We investigated the effect of applying electric field pulses during both the dephasing (t_{12}) period and the rephasing (t_{23}) period. If identical electric field pulses are applied during these two periods the echo amplitude is unaffected since both sets of ions have the same phase shift applied. If, on the other hand, the sign of the pulse amplitude is changed in the second period, the phase shifts in the two periods add. We applied the pair of pulses in the form of a full cycle of a sine wave with a period of $100\ \mu\text{s}$ as shown in Fig. 5(a). The first minimum in the echo intensity (π phase shift) occurred at 30 mV p-p and the second (3π phase shift) at 90 mV p-p [Fig. 5(b)]. In a second experiment a rectangular pulse was applied only during the period t_{12} . The ratio of the area of a half cycle of a sine pulse and a rectangular pulse of the same height and width is $2/\pi$. A rectangular pulse of amplitude $2/\pi$ times 30 mV produced the same π phase shift as the two half cycles of

the sine pulse, showing that the phase shifts during the two half periods of the sine pulse added. The two experiments gave the same Stark coefficient of 27 kHz cm/V for the field along $D1$ as shown in Fig. 5(c). This Stark coefficient was also measured by Graf *et al.* [26] who found a total magnitude for the dipole moment difference of 35 kHz cm/V . From this, the angle between the vector dipole moment difference and $D1$ is $\cos^{-1}(0.77) = 40^\circ$.

We measured the Stark effect of the nuclear quadrupole levels of a partly filled f -shell system: ^{151}Eu in Y_2SiO_5 single crystals. The magnitudes of the Stark shifts are $\sim 1\text{ Hz cm/V}$. Measurements of these small shifts, using small electric fields on very dilute systems were made possible by combining optical Raman heterodyne detection with Stark modulated nuclear quadrupole echoes. Unlike the case of electronic states the nuclear quadrupole levels do not have an electric dipole moment and the Stark effect results from the nuclear quadrupole moment sensing the linear change in the electric field gradient induced by the applied electric field. In the case of the optical electronic transitions, the electric field produces a change in the electric dipole moment which is different in the ground and excited states. The frequency shift in the latter case is $>10^4$ times larger than for the nuclear levels. The sensitivity of our measurement method was sufficient to observe Stark shifts that were as small as 20 ppm of the quadrupole resonance inhomogeneous line widths and 1 part in 10^8 of the NQR frequency, using only very small applied electric fields. Schemes to increase the decoherence times of the nuclear spin states [7–9] will lead to further substantial increases in the sensitivity of these measurements. Higher fields would make it possible to observe shifts that are several times the inhomogeneous width and perhaps also extend the technique of Stark switched coherent transients [27] to the nuclear levels.

The authors thank M. Lovrić for designing the Raman heterodyne apparatus and J.-F. Engrand for technical assistance. R.M.M. would like to thank Philippe Goldner for his hospitality in his lab at the Institut de Recherche de Chimie Paris where the experiments were carried out. This work was funded in part by the European Union’s Seventh Framework Program, FP7/2007-2013/ under REA Grant Agreements No. 287252 (CIPRIS, People Program-Marie Curie Actions).

*macfarla@us.ibm.com

†Present address: NEST, Scuola Normale Superiore and Istituto Nanoscienze-CNR, Piazza San Silvestro 12, 56127 Pisa, Italy.

andrea.arcangeli@nano.cnr.it

‡philippe.goldner@chimie-paristech.fr

[1] D. Rieländer, K. Kutluer, P. M. Ledingham, M. Gündoğan, J. Fekete, M. Mazzera, and H. de Riedmatten, *Phys. Rev. Lett.* **112**, 040504 (2014).

- [2] H. de Riedmatten, M. Afzelius, M. U. Staudt, C. Simon, and N. Gisin, *Nature (London)* **456**, 773 (2008).
- [3] M. P. Hedges, J. J. Longdell, Y. Li, and M. J. Sellars, *Nature (London)* **465**, 1052 (2010).
- [4] C. Clausen, I. Usmani, F. Bussi eres, N. Sangouard, M. Afzelius, H. de Riedmatten, and N. Gisin, *Nature (London)* **469**, 508 (2011).
- [5] E. Saglamyurek, N. Sinclair, J. Jin, J. A. Slater, D. Oblak, F. Bussi eres, M. George, R. Ricken, W. Sohler, and W. Tittel, *Nature (London)* **469**, 512 (2011).
- [6] F. Bussi eres, C. Clausen, A. Tiranov, B. Korzh, V. B. Verma, S. W. Nam, F. Marsili, A. Ferrier, P. Goldner, H. Herrmann, C. Silberhorn, W. Sohler, M. Afzelius, and N. Gisin, *Nat. Photonics* (to be published).
- [7] C. Yin, M. Rancic, G. G. de Boo, N. Stavrias, J. C. McCallum, M. J. Sellars, and S. Rogge, *Nature (London)* **497**, 91 (2013).
- [8] P. Siyushev, K. Xia, R. Reuter, M. Jamali, N. Zhao, N. Yang, C. Duan, N. Kukharchyk, A. D. Wieck, R. Kolesov, and J. Wrachtrup, *Nat. Commun.* **5**, 3895 (2014).
- [9] E. Fraval, M. J. Sellars, and J. J. Longdell, *Phys. Rev. Lett.* **92**, 077601 (2004).
- [10] E. Fraval, M. J. Sellars, and J. J. Longdell, *Phys. Rev. Lett.* **95**, 030506 (2005).
- [11] M. Lovri c, D. Suter, A. Ferrier, and P. Goldner, *Phys. Rev. Lett.* **111**, 020503 (2013).
- [12] J. Stark, *Sitzungsber. K. Preuss. Akad. Wiss. Berlin* **47**, 932 (1913).
- [13] J. Mlynek, N. C. Wong, R. G. DeVoe, E. S. Kintzer, and R. G. Brewer, *Phys. Rev. Lett.* **50**, 993 (1983); N. C. Wong, E. S. Kintzer, J. Mlynek, R. G. DeVoe, and R. G. Brewer, *Phys. Rev. B* **28**, 4993 (1983).
- [14] W. B. Mims, *Phys. Rev.* **133**, A835 (1964).
- [15] N. E. Ainbinder and Yu. G. Svetlov, *Zh. Strukt. Khim.* **14**, 766 (1973) [*J. Struct. Chem.* **14**, 721 (1974)].
- [16] T. Kushida and K. Saiki, *Phys. Rev. Lett.* **7**, 9 (1961).
- [17] J. Armstrong, N. Bloembergen, and D. Gill, *Phys. Rev. Lett.* **7**, 11 (1961).
- [18] F. P. Raghavan, *At. Data Nucl. Data Tables* **42**, 189 (1989).
- [19] W. M oller, H. H uhnermann, G. Alkhozov, and V. Panteleev, *Phys. Rev. Lett.* **70**, 541 (1993).
- [20] R. J. Elliott, *Proc. Phys. Soc. London Sect. B* **70**, 119 (1957).
- [21] R. Yano, M. Mitsunaga, and N. Uesugi, *J. Opt. Soc. Am. B* **9**, 992 (1992).
- [22] R. Yano, M. Mitsunaga, and N. Uesugi, *Opt. Lett.* **16**, 1884 (1991).
- [23] B. Lauritzen, N. Timoney, N. Gisin, M. Afzelius, H. de Riedmatten, Y. Sun, R. M. Macfarlane, and R. L. Cone, *Phys. Rev. B* **85**, 115111 (2012).
- [24] A. J. Meixner, C. M. Jefferson, and R. M. Macfarlane, *Phys. Rev. B* **46**, 5912 (1992).
- [25] E. S. Kintzer, M. Mitsunaga, and R. G. Brewer, *Phys. Rev. B* **31**, 6958 (1985).
- [26] F. R. Graf, A. Renn, G. Zumofen, and U. P. Wild, *Phys. Rev. B* **58**, 5462 (1998).
- [27] G. Brewer and R. L. Shoemaker, *Phys. Rev.* **A6**, 2001 (1972).